PHYSICAL REVIEW D **80,** 071503(R) (2009)

Efficient simulation of relativistic fermions via vertex models

Urs Wenger

Institute for Theoretical Physics, University of Bern, Sidlerstrasse 5, CH-3012 Bern, Switzerland

(Received 1 June 2009; published 29 October 2009)

We have developed an efficient simulation algorithm for strongly interacting relativistic fermions in two-dimensional field theories based on a formulation as a loop gas. It essentially eliminates critical slowing down by sampling two-point correlation functions and allows simulations directly in the massless limit at the critical point. It generates loop configurations with fluctuating topological boundary conditions enabling one to simulate fermions with arbitrary periodic or antiperiodic boundary conditions. As illustrative examples, the algorithm is applied to the Gross-Neveu model and to the Schwinger model in the strong coupling limit.

DOI: 10.1103/PhysRevD.80.071503 PACS numbers: 11.15.Ha, 02.70.−c, 05.50.+q

Simulating strongly interacting fermions, like in quantum chromodynamics (QCD) or in Nambu-Jona–Lasinio models, is considered to be rather difficult and continues to be a challenge due to the nonlocality of the determinant obtained upon integrating out the fermionic fields. Moreover, simulations of fermions are usually hampered by critical slowing down towards the chiral limit where the fermions become massless and the correlation length of the fermionic two-point function diverges. The established standard method to perform such calculations on the lattice is to use the hybrid Monte Carlo algorithm [1] which deals with the nonlocality of the determinant by rewriting it as an integral over bosonic ''pseudofermion'' fields. The algorithm then requires one to deal with the inverse of the fermion Dirac operator, however, the operator becomes ill-conditioned towards the massless limit and the simulations slow down dramatically. In this paper we propose a novel approach which circumvents the above mentioned problems. It is based on a (high-temperature) expansion of the fermion actions which reformulates the fermionic systems as q-state vertex models, i.e., statistical closed loop models. In particular, the method is directly applicable to the Gross-Neveu (GN) model and to the Schwinger model in the strong coupling limit. These models can be shown to be equivalent to specific vertex models [2–5] and our simulation method, based on a proposal by Prokof'ev and Svistunov [6], is effectively a very efficient updating algorithm for generic vertex models (in arbitrary dimensions). In fact, the algorithm essentially eliminates critical slowing down and is able to simulate the fermionic systems at the critical point and directly in the massless limit.

We start with illustrating the reformulation in terms of closed loops in the GN model. The model is most naturally formulated by employing Majorana fermions [7,8]. Here we are using Wilson's Euclidean lattice discretization for which the action density of the model is

$$\mathcal{L}_{\mathrm{GN}} = \frac{1}{2}\xi^T\mathcal{C}\left(\gamma_\mu\tilde{\partial}_\mu - \frac{1}{2}\partial^*\partial + m\right)\xi - \frac{g^2}{4}(\xi^T\mathcal{C}\xi)^2, \quad (1)$$

where ξ is a real, two component Grassmann field describing a Majorana fermion with mass m, $\mathcal{C} = -\mathcal{C}^T$ is the charge conjugation matrix, and ∂, ∂^*, $\tilde{\partial}$ denote the forward, backward and symmetric lattice derivative, respectively. The Wilson term $\frac{1}{2}\partial^*\partial$, responsible for removing the fermion doublers, explicitly breaks the discrete chiral symmetry $\xi \to \gamma_5\xi$, $\xi^T\mathcal{C} \to \xi^T\mathcal{C}\gamma_5$ and requires a fine-tuning of $m \to m_c$ towards the continuum limit in order to restore the symmetry. A pair ξ_1, ξ_2 of Majorana fermions may be considered as one Dirac fermion using the identification $\psi = \frac{1}{\sqrt{2}}(\xi_1 + i\xi_2)$, $\bar{\psi} = \frac{1}{\sqrt{2}}(\xi_1^T - i\xi_2^T)\mathcal{C}$ and the corresponding GN model with N Dirac fermions has an $O(2N)$ flavor symmetry. At $g = 0$, integrating out the Grassmann variables yields the partition function in terms of the Pfaffian

$$Z_{\mathrm{GN}} = \mathrm{Pf}\left[\mathcal{C}\left(\gamma_\mu\tilde{\partial}_\mu + m - \frac{1}{2}\partial^*\partial\right)\right]^{2N}. \quad (2)$$

For $g \neq 0$ one usually performs a Hubbard-Stratonovich transformation and introduces a scalar field σ conjugate to $\xi^T\mathcal{C}\xi$ together with an additional Gaussian Boltzmann factor $\exp\{-1/(2g^2)\sum_x\sigma(x)^2\}$ for the scalar field.

In order to reformulate the model in terms of closed loops (or equivalently dimers and monomers) we follow the recent derivation of Wolff [8] (see [4,5] for alternative, but more complicated derivations). One simply expands the Boltzmann factor for the fermionic fields and makes use of the nil-potency of the Grassmann variables upon integration. Introducing $\varphi(x) = 2 + m + \sigma(x)$ and the projectors $P(\pm\mu) = (1 \mp \gamma_\mu)/2$ we can write the fermionic part of the GN path integral (up to an overall sign) as

$$\int \mathcal{D}\xi \prod_x (\varphi(x)\xi^T(x)\mathcal{C}\xi(x))^{m(x)} \times \prod_{x,\mu} (\xi^T(x)\mathcal{C}P(\mu)\xi(x+\hat{\mu}))^{b_\mu(x)} \quad (3)$$

where $m(x) = 0, 1$ and $b_\mu(x) = 0, 1$ are the monomer and bond (or dimer) occupation numbers, respectively. Integration over the fermion fields yields the constraint that at each site $m(x) + \frac{1}{2}\sum_\mu b_\mu(x) = 1$. Here the sum

runs over positive and negative directions and $b_{-\mu}(x) = b_\mu(x - \hat{\mu})$. The constraint ensures that only closed and nonintersecting loops of occupied bonds contribute to the partition function and also accounts for the fact that the loops are nonbacktracking, a consequence of the orthogonal projectors $P(\pm\mu)$. The weight $\omega(\ell)$ of each loop ℓ can be calculated analytically [9] and yields $|\omega(\ell)| = 2^{-n_c/2}$ where n_c is the number of corners along the loop. The sign of ω will generically depend on the geometrical shape of the loop [9] prohibiting a straightforward probabilistic interpretation of the loop weights in dimensions $d > 2$.

In two dimensions, however, the sign of the loop only depends on the topology of the loop and is determined by the fermionic boundary conditions (BC). This has been well known for a long time [10] but has recently been clarified by Wolff [8] in the context of the GN model. It is therefore useful to classify all loop configurations into the four equivalence classes $\mathcal{L}_{00}$, $\mathcal{L}_{10}$, $\mathcal{L}_{01}$, $\mathcal{L}_{11}$ where the index denotes the total winding (modulo two) of the loops in the two directions. The weights of all configurations in $\mathcal{L}_{10}$ and $\mathcal{L}_{11}$ for example will pick up an overall minus sign if we change the fermionic boundary condition in the first direction from periodic to antiperiodic, while the weights of the configurations in $\mathcal{L}_{00}$ and $\mathcal{L}_{01}$ remain unaffected. As a consequence, if we sum over all the topological equivalence classes with positive weights, i.e., $Z \equiv Z_{\mathcal{L}_{00}} + Z_{\mathcal{L}_{10}} + Z_{\mathcal{L}_{01}} + Z_{\mathcal{L}_{11}}$ we effectively describe a system with unspecified fermionic boundary conditions. Vice versa, the partition function $Z_\xi^{10} \equiv Z_{\mathcal{L}_{00}} + Z_{\mathcal{L}_{10}} - Z_{\mathcal{L}_{01}} + Z_{\mathcal{L}_{11}}$, e.g., describes a system with fermionic BC antiperiodic in the first and periodic in the second direction.

It is useful to point out the equivalence of the loop gas formulation to the 8-vertex model [11,12] which is formulated in terms of the eight vertex configurations shown in the top row of Fig. 1 with weights ω_i, $i = 1, \ldots, 8$. The partition function is defined as the sum over all possible tilings of the square lattice with the eight vertices such that only closed (but possibly intersecting) paths occur. To be precise, one has

$$Z_{\text{8-vertex}} = \sum_{\text{CP}} \prod_x \omega_i(x), \tag{4}$$

where the sum is over all closed path configurations (CP) and the weight of each configuration is given by the product of all vertex weights in the configuration. For the GN model we have the following weights

$$\omega_1 = \varphi(x), \qquad \omega_2 = 0, \qquad \omega_3 = \omega_4 = 1, \qquad \omega_5 = \omega_6 = \omega_7 = \omega_8 = \frac{1}{\sqrt{2}}, \tag{5}$$

i.e. each corner contributes a factor $1/\sqrt{2}$, while crossings of two lines are forbidden ($\omega_2 = 0$) and each empty site carries the monomer weight $\omega_1 = \varphi(x)$.

The GN model with a single Majorana fermion is effectively a free fermion system and we use it as a benchmark to compare the results of our algorithm with analytic results. Instances of the 8-vertex model for which no analytic solutions are known include the Ising model with additional next-to-nearest-neighbor and quartic interactions [13]. The one-flavor Schwinger model with Wilson fermions in the strong coupling limit is an 8-vertex model with a fermionic interpretation [2,14]. The vertex weights are given by

$$\omega_1 = (m+2)^2, \qquad \omega_2 = 0, \qquad \omega_3 = \omega_4 = 1, \qquad \omega_5 = \omega_6 = \omega_7 = \omega_8 = \frac{1}{2}, \tag{6}$$

where the monomer weight and the corner weights are squared due to the fact that we are dealing with a pair of Majorana fermions glued together [15].

Let us now turn to the description of the new method to efficiently simulate any vertex model in arbitrary dimensions with generic (positive) weights ω_i, including the fermionic models discussed above. For illustrative purpose we restrict the discussion to the 8-vertex model. The method is an extension of the so-called worm algorithm by Prokof'ev and Svistunov [6]. The configuration space of closed loops is enlarged to also contain open strings. For the GN model such an open string with ends at x and y corresponds to the insertion of two Majorana fields at positions x and y which is simply the Majorana fermion propagator

$$G(x, y) = \int \mathcal{D}\xi e^{-S_{\text{GN}}} \xi(x)\xi(y)^T \mathcal{C}. \tag{7}$$

Similar interpretations of the open string can be obtained for other vertex models. The open string is now the basis for a Monte Carlo algorithm which samples directly the space of 2-point correlation functions instead of the standard configuration space. This is the reason why the algorithm is capable of beating critical slowing down as demonstrated below: at a critical point where the correlation length grows large, the configurations are updated equally well on all length scales up to a scale of the order of the correlation length.

In the vertex language the insertions correspond to the new vertex configurations depicted in the bottom row of

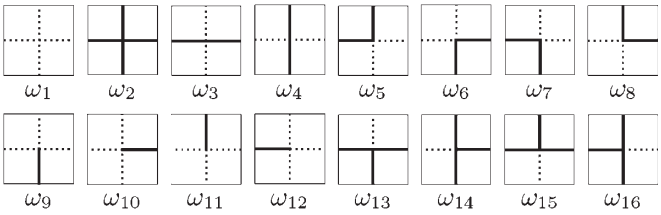

FIG. 1. The vertex configurations and weights of the eight-vertex model (top row) and the extended model (bottom row).

Fig. 1. A configuration containing a single open string corresponds to a loop configuration with two instances of vertex 9–16 which are connected by a string. Note that vertices 13–16, while present in the generic extended vertex model, do not have a physical interpretation in terms of fermionic fields since they are explicitly forbidden by Pauli's exclusion principle (fermionic lines are not allowed to intersect). Nevertheless they can also be included in the fermionic models, simply for algorithmic efficiency, and we do so in our implementation.

The algorithm now proceeds by locally updating the ends of the open string using a simple Metropolis or heat bath step according to the weights of the corresponding 2-point function. When one end is shifted from, say, x to one of its neighboring points y, a dimer on the corresponding bond is destroyed or created depending on whether the bond is occupied or not. In the process, the two vertices at x and y are changed from v_x, v_y to v'_x, v'_y and the move is accepted with probability

$$P(x \to y) = \min\left[1, \frac{\omega_{v'_x}}{\omega_{v_x}} \frac{\omega_{v'_y}}{\omega_{v_y}}\right] \tag{8}$$

in order to satisfy detailed balance. So a global update results from a sequence of local moves, and in this sense it is similar in spirit to the loop cluster update [16], the directed loop algorithm [17] or the directed path algorithm for constrained monomer-dimer systems [18].

Whenever the two ends of the open string meet, a new closed loop is formed and the new configuration contributes to the original partition function Z in one of the classes $\mathcal{L}_{00}, \mathcal{L}_{10}, \mathcal{L}_{01}, \mathcal{L}_{11}$. In this way the overall normalization is ensured, and expectation values can be calculated as usual. The algorithm switches between the topological sectors with ease: as the string evolves it can grow or shrink in any direction and wrap around the torus. Effectively, the algorithm simulates a system with fluctuating topological boundary conditions.

In principle, the weight of the open string can be chosen arbitrarily, but the physical interpretation in Eq. (7) suggests to choose the weights ω_9 to ω_{16} such that the open string configurations sample directly the 2-point correlation function, hence providing an improved estimator. During the simulation one simply updates a table for $G(x, y)$ as the string end points move around and the expectation value is obtained by forming $\langle G(x, y)\rangle_Z = G(x, y)/Z$.

For the fermionic models we also need to keep track of the Dirac structure associated with $G(x, y)$. This is most easily done by adding the product of the Dirac projectors along the string ℓ, i.e. $\prod_{\mu\in\ell} P(\mu)$, as a contribution at each step. Care has to be taken when the open string winds an odd times around a boundary on which we want to impose antiperiodic boundary conditions for the fermions. In that case we need to account for an additional minus sign in the contribution to $G(x, y)$. For the fermionic models where vertices 13–16 have no physical meaning, the weights ω_{13} to ω_{16} can be tuned for algorithmic efficiency and do not follow any physically inspired rule. A good choice is to use the geometric mean of the weights ω_i of those vertices that can be reached in one further update step, e.g. $\omega_{13} = (\omega_4\omega_6\omega_7)^{1/3}$. Finally, let us emphasize again that the algorithm described here is applicable to any vertex model, also in higher dimensions, as long as the weights are positive definite in well-defined configuration classes.

We have performed extensive tests of our algorithm by comparing to exact results known from Pfaffians (for the Majorana GN model) or from explicit calculations on small lattices. Simple observables are linear combinations of partition functions and ratios thereof, e.g. $Z_{\mathcal{L}_{ij}}/Z$ with $i, j = 0, 1$. In Fig. 2 we show the results for the ratios $Z_{\mathcal{L}_{ij}}/Z$ in the Majorana GN model on a 128^2 lattice as a function of the bare mass m. Dashed lines are the exact results calculated from the Pfaffians. Note that all partition function ratios are obtained in the same simulation. In the inset we also show the ratio Z^{00}_ξ/Z where $Z^{00}_\xi \equiv Z_{\mathcal{L}_{00}} - Z_{\mathcal{L}_{01}} - Z_{\mathcal{L}_{10}} - Z_{\mathcal{L}_{11}}$ is the partition function with fermionic BC periodic in space and time direction. In that situation the Majorana Dirac operator has a zero mode at $m = 0$ (and at $m = -2$) and the system is critical. The inset in Fig. 2 illustrates that the algorithm can reproduce this zero mode without problems and that we can in fact simulate directly at the critical point. Conversely, we can use $Z^{00}_\xi/Z = 0$ as a definition of the critical point $m = m_c$. In Fig. 3 we show our results for Z^{00}_ξ/Z as a function of the bare mass m in the Schwinger model in the strong coupling limit for various volumes. The critical point can be determined accurately with very little computational effort and we obtain $m_c = -0.686\,506(27)$ (cf. inset in Fig. 3) from

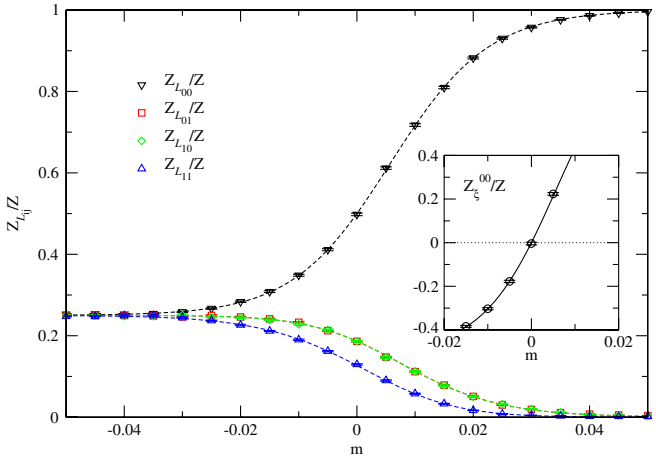

FIG. 2 (color online). Results for the ratios $Z_{\mathcal{L}_{ij}}/Z$ for the Majorana GN model on a 128^2 lattice as a function of the bare mass m. Dashed lines are the exact results. The inset shows Z^{00}_ξ/Z and illustrates how the zero mode at $m = 0$ is reproduced.

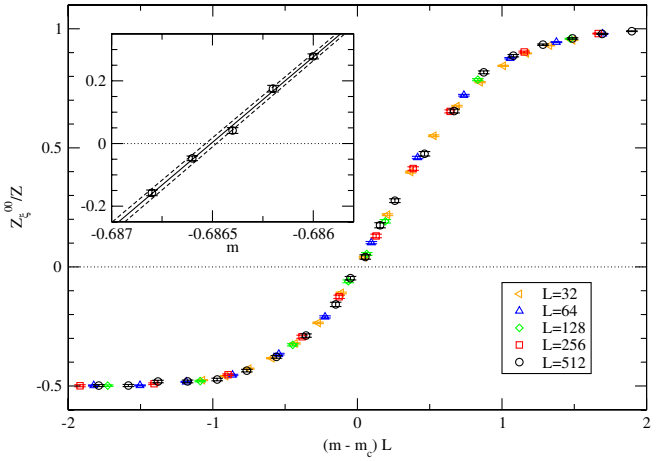

FIG. 3 (color online). Finite size scaling data collapse of Z_ξ^{00}/Z in the Schwinger model at strong coupling consistent with a second order phase transition with critical exponent $\nu = 1$). The inset shows the determination of the critical mass $m_c = -0.686\,506(27)$ from a linear interpolation of the data on the largest lattice with $L = 512$.

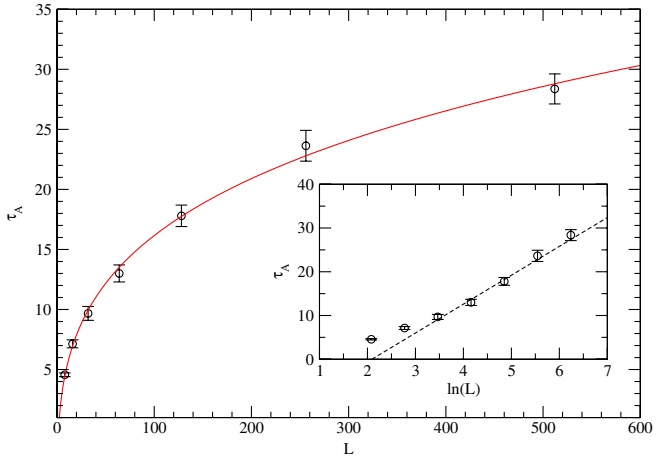

FIG. 4 (color online). Integrated autocorrelation time τ_A of the energy for the Schwinger model in the strong coupling limit at the critical point $m = m_c$. The line is a fit $\tau_A \propto L^z$ yielding $z = 0.25(2)$. The inset shows the logarithmic dependence $-18(3) + 7.5(6)\ln(L)$ from fitting to $L \geq 64$.

our simulations on the largest lattice with $L = 512$. Further improvement could be achieved by employing standard reweighting techniques as done in [19] where they obtained $m_c = -0.6859(4)$. These calculations indicated a second order phase transition in the universality class of the Ising model (with critical exponent $\nu \simeq 1$). Our results in Fig. 3 now confirm this by demonstrating that the partition function ratios Z_ξ^{00}/Z as a function of the rescaled mass $(m - m_c)L^\nu$ with $\nu = 1$ beautifully collapse onto a universal scaling curve.

The efficiency of the algorithm and the fact that critical slowing down is essentially absent is demonstrated in Fig. 4 where we show the integrated autocorrelation time τ_A of the energy as a function of the linear system size L at the critical point $m = m_c$. (Similar plots can be obtained for the Majorana GN model.) The functional dependence on L can be well fitted (χ^2/d.o.f. $= 1.28$) by $\tau_A \propto L^z$ all the way down to our smallest system size $L = 8$. We obtain $z = 0.25(2)$ which is consistent with just using the largest two system sizes. It is an amazing result that our local Metropolis-type update appears to have a dynamical critical exponent close to zero. The autocorrelation time may also depend logarithmically on L and a fit to $L \geq 64$ yields $-13.8(1.9) + 6.6(4)\ln(L)$ with χ^2/d.o.f. $= 1.00$.

In conclusion, we have presented a new type of algorithm for generic vertex models. It relies on sampling directly 2-point correlation functions and essentially eliminates critical slowing down. We have successfully tested our algorithm on the Majorana GN model and on the Schwinger model in the strong coupling limit and found remarkably small dynamical critical exponents. The algorithm definitely opens the way to simulate efficiently generic vertex models (with positive weights) in arbitrary dimensions, in particular the GN model with any number of flavors, the Thirring model, the Schwinger model and QED_3 in the strong coupling limit, as well as fermionic models with Yukawa-type scalar interactions, all with Wilson fermions.

I would like to thank Philippe de Forcrand and Michael Fromm for useful and sometimes crucial discussions. This work is supported by SNF Grant No. PP002-_119015.

Note added.—The technical details of our proposal have also been worked out independently in [20] which appeared while we finalized this paper.

[1] S. Duane, A. D. Kennedy, B. J. Pendleton, and D. Roweth, Phys. Lett. B **195**, 216 (1987).
[2] M. Salmhofer, Nucl. Phys. **B362**, 641 (1991).
[3] K. Scharnhorst, Nucl. Phys. **B479**, 727 (1996).
[4] K. Scharnhorst, Nucl. Phys. **B503**, 479 (1997).
[5] C. Gattringer, Nucl. Phys. **B543**, 533 (1999).
[6] N. Prokof'ev and B. Svistunov, Phys. Rev. Lett. **87**, 160601 (2001).
[7] C. Itzykson and J. M. Drouffe, *Statistical Field Theory* (Cambridge University Press, Cambridge, England, 1989), Vol. 2.
[8] U. Wolff, Nucl. Phys.**B789**, 258 (2008).

[9] I. O. Stamatescu, Phys. Rev. D **25**, 1130 (1982).
[10] P. W. Kasteleyn, Physica (Amsterdam) **27**, 1209 (1961).
[11] B. Sutherland, J. Math. Phys. (N.Y.) **11**, 3183 (1970).
[12] C. Fan and F. Y. Wu, Phys. Rev. B **2**, 723 (1970).
[13] R. J. Baxter, *Exactly Solved Models in Statisticals Mechanics* (Academic, London, 1982).
[14] C. Gattringer, Nucl. Phys. **B559**, 539 (1999).
[15] One can in fact derive these weights also for $d = 3$ and show that all loop contributions are positive, hence allowing simulations of QED_3 in the strong coupling limit.
[16] H. G. Evertz, G. Lana, and M. Marcu, Phys. Rev. Lett. **70**, 875 (1993).
[17] O. F. Syljuasen and A. W. Sandvik, Phys. Rev. E **66**, 046701 (2002).
[18] D. H. Adams and S. Chandrasekharan, Nucl. Phys. **B662**, 220 (2003).
[19] H. Gausterer and C. B. Lang, Nucl. Phys. **B455**, 785 (1995).
[20] U. Wolff, Nucl. Phys. **B814**, 549 (2009).